ANNUAL OF NAVIGATION 6/2003

Jaroslaw Artyszuk
Szczecin Maritime University

A NOVEL METHOD OF SHIP MANOEUVRING MODEL IDENTIFICATION FROM SEA TRIALS

ABSTRACT The ship manoeuvring dynamics consists of surge, sway, and yaw differential equations (coupled mutually with each other). a basic principle of the proposed manoeuvring model identification algorithm is that both sway and yaw equations may directly assimilate, instead of the motions derived from other one or two equations, the corresponding sea trial data. Under such conditions, the evaluated hull and rudder sub-models are more adequate and less ambiguous. An approach has been made also to compose the hull hydrodynamics from turning tests, while z-tests refine the rudder related model parameters. The obtained final manoeuvring prediction is excellent.

INTRODUCTION

Difficulties in achieving a rather well physically validated correction factor for the rudder inflow lateral velocity due to the manoeuvring ship hull interaction, e.g. [Artyszuk, 1999, 2001a, 2002] have been mainly caused by a too high role of the sway added mass in the surge motion equation. Much better and hydrodynamically more justified results would be obtained by introducing a correction multiplier for the sway added mass, but only (what is important) in the surge equation (the other two sway and yaw equations include also the sway added mass). Though some scale model tests confirm such an interference in certain limits (as associated with the ship hull positive thrust being generated by the sway/yaw manoeuvring motions), they rarely state that a drastic decrease of the sway added mass significance is often necessary. The latter sometimes means a much more critical figure than usually reported 80% for a full form ship like e.g. a tanker. Much lower values approx. 50% are frequently cited for slender ships. In the present study, a case of the disappearing sway added mass in the surge equation is considered.

Moreover, many other sound conclusions towards the ship manoeuvring model structural identification in the sway and yaw equations, as drawn just from the analysis of the surge motion equation, are often too exaggerated due to some errors in the manoeuvring trials and not adequate assumptions behind the manoeuvring model itself.

Such circumstances has directed the author's attention to the ship manoeuvring model identification process, in which the surge velocity in both sway and yaw equations comes from the sea manoeuvring trials. The progress in the ship manoeuvring model identification is really crucial here. The present work shows details of such an approach.

A chemical tanker of data presented in Tab. 1 is used as an example.

Table 1. Ship particulars

type:	chemical tanker	MAIN ENGINE:	
DWT	6000[t]	type:	diesel
HULL:		P_{En}	3600[kW]
m	8950[t]	n_n	146[rpm]
J_z	$5.2\cdot10^6$[tm^2]	PROPELLER:	
m_{11}	6%m	type:	CPP
m_{22}	100%m	D	4.1[m]
m_{66}	83%J_z	$(P/D)_n$	0.8719
L	97.4[m]	RUDDER:	
B	16.6[m]	type:	Schilling
T	7.1[m]	A_R	12.3[m^2]
c_B	0.76[-]	λ	1.5[-]

MANOEUVRING MATHEMATICAL MODEL BASIC FORMULATION

The ship manoeuvring differential equations in a practically accepted form are written as follows (the ship-fixed system of reference):

$$\begin{cases} \dfrac{dv_x}{dt}\left(m+m_{11}\right) & = +\left(m+\underline{c_m}m_{22}\right)v_y\omega_z+F_x \\ \dfrac{dv_y}{dt}\left(m+m_{22}\right) & = -\left(m+m_{11}\right)v_x\omega_z+F_y \\ \dfrac{d\omega_z}{dt}\left(J_z+m_{66}\right) & = -\left(m_{22}-m_{11}\right)v_xv_y+M_z \end{cases} \tag{1}$$

where c_m constant represents the mentioned hull positive thrust as produced by the hull drift/yaw manoeuvring motions and not being normally contained in the hull resistance F_{xH} component (dependent mostly on the surge velocity v_x). This semi-empirical constant shall be paid more and more attention in the future manoeuvring research field, since it greatly enables a good convergence of full-scale trials and the mathematical model simulations.

There are different estimates of the c_m coefficient in the open literature as has been mentioned in the introduction chapter, but more data are still required. In the specific case of the chemical tanker being investigated hereafter, the analysis of manoeuvring behaviour during crash stopping and coasting sea trials, as strongly affected by drift/yaw motions due to a propeller lateral thrust, leads to a nearly zero value for c_m. And this will be further taken as the reference.

The below models (frameworks) of particular external excitations are adopted in the present identification study:

$$\begin{cases} F_x &= F_{xH} + F_{xP} + F_{xR} \\ F_y &= F_{yH} + F_{yR} \\ M_z &= M_{zH} + x_R F_{yR} \end{cases} \tag{2}$$

hull forces:

$$\begin{bmatrix} F_{xH} \\ F_{yH} \\ M_{zH} \end{bmatrix} = 0.5\rho LT\left(v_{xy}^2 + \omega_z^2 L^2\right) \begin{bmatrix} c_{fxhm}(\beta, \Omega_m) \\ c_{fyhm}(\beta, \Omega_m) \\ Lc_{mzhm}(\beta, \Omega_m) \end{bmatrix} \tag{3}$$

$$v_{xy} = \sqrt{v_x^2 + v_y^2}\,,\ \mathrm{arctg}\beta = \frac{-v_y}{v_x}\,,\ \beta \in \left(-180°, +180°\right\rangle \tag{4}$$

$$\Omega_m = \frac{\omega_z L}{\sqrt{v_{xy}^2 + \omega_z^2 L^2}}\,,\ \Omega_m \in \left\langle -1, +1 \right\rangle \tag{5}$$

propeller forces:

$$F_{xP} = (1-t)T_P = (1-t)\rho D^2\left(v_p^2 + n^2 D^2\right)k_{tm}\left(J_m, P/D\right) \tag{6}$$

$$v_p = v_x(1-w),\ J_m = \frac{nD}{\sqrt{v_p^2 + n^2 D^2}}\,,\ J_m \in \left\langle -1, +1 \right\rangle \tag{7}$$

rudder forces:

$$\begin{bmatrix} F_{xR} \\ F_{yR}^{*} \end{bmatrix} = \begin{bmatrix} \cos(-\beta_R) & -\sin(-\beta_R) \\ \sin(-\beta_R) & \cos(-\beta_R) \end{bmatrix} \begin{bmatrix} F_{DR} \\ F_{LR} \end{bmatrix}, \; F_{yR} = F_{yR}^{*}\left(1 + \underline{a_H}\right) \tag{8}$$

$$\begin{bmatrix} F_{DR} \\ F_{LR} \end{bmatrix} = 0.5\rho A_R v_R^2 \begin{bmatrix} c_D(\alpha, c_{Th}) \\ c_L(\alpha, c_{Th}) \end{bmatrix}, \; \alpha = \delta + \beta_R, \; c_{Th} = \frac{T_P}{0.5\rho \frac{\pi D^2}{4} v_p^2} \tag{9}$$

$$\mathrm{tg}\,\beta_R = -v_{yR} / v_{PS}, \; v_{yR} = \underline{c_{12}}\left(v_y + \omega_z x_R\right) \tag{10}$$

$$v_R = \sqrt{v_{PS}^2 + v_{yR}^2}, \; v_{PS} = \sqrt{v_p^2 + \frac{8T_P}{\rho \pi D^2}} \tag{11}$$

The hull resistance coefficient c_{fxhm} in (3) may be derived by a simple transformation of the following practical relationship:

$$F_{xH} = 0.5\rho L T v_{xy}^2 \cos\beta \cdot \underbrace{c_{fxh0}}_{<0} \tag{12}$$

where c_{fxh0} is the traditional hull resistance coefficient in ahead motion.

Hence:

$$c_{fxhm} = c_{fxh0} \cdot \cos\beta \cdot \left(1 - \Omega_m^2\right) \tag{13}$$

The propeller thrust coefficient k_{tm} is recalculated on the basis of controllable pitch propeller characteristics supplied in [Ruseckij, 1968]. The manoeuvring model being examined comprises also a decrease of pitch or revolutions due to the main engine overload, the appropriate expressions are not however cited here.

The rudder force lift c_L and drag c_D coefficients are illustrated in Fig. 1 for the specific Schilling-type rudder installed on the chemical tanker in concern. a method of their construction has been explained in [Artyszuk, 2001b].

The a_H parameter is often introduced due to the hull-rudder interaction as reflecting an additional transverse force produced on the ship hull while a deflection of the rudder. The a_H coefficient is mainly assumed constant, though its nature is frequently reported as being much more complex. In the particular case of the adopted Schilling rudder hydrodynamics (Fig. 1), the a_H parameter will also enable 'hiding' some deficiencies of the lift/drag charts.

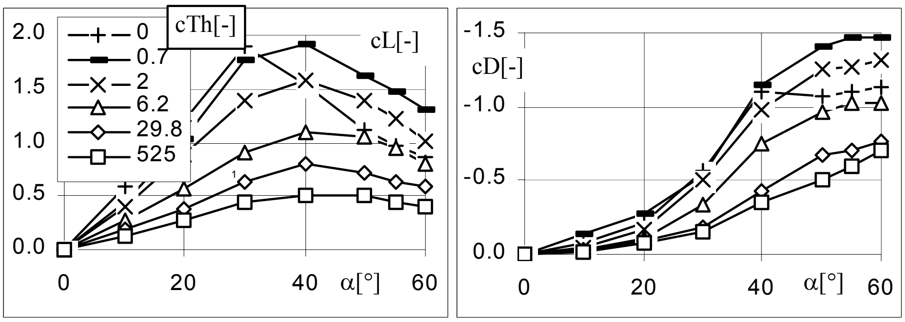

Fig. 1. Rudder lift/drag coefficients

The c_{12} factor plays a role of modelling the so-called effective rudder local drift. a constant value is also assumed here as the early approximation.

An initial guess for the hull sway force c_{fyhm} and yaw moment c_{mzhm} coefficients is written according to two simple (but realistic enough) background relationships:

$$\begin{bmatrix} F_{yH} \\ M^{*}_{zH} \end{bmatrix} = 0.5\rho L T v_{xy}^{2} \begin{bmatrix} c_{fyh}\left(\beta, \overline{\omega_z}\right) \\ c_{mzh}\left(\beta, \overline{\omega_z}\right) \end{bmatrix}, \quad \overline{\omega_z} = \frac{\omega_z L}{v_{xy}} \tag{14}$$

$$M_{zH} = M^{*}_{zH} + \left(m_{22} - m_{11}\right) v_x v_y \tag{15}$$

where for the chemical tanker (see also [Artyszuk, 2003b]):

$$\begin{cases} c_{fyh} & = & +0.5\sin\beta + 0.6\left|\overline{\omega_z}\right| \\ c_{mzh} & = & +0.1\sin 2\beta - 0.07\left|\overline{\omega_z}\right|\overline{\omega_z} \end{cases} \tag{16}$$

The conversion of c_{fyh} and c_{mzh} into c_{fyhm} and c_{mzhm} is rather easy. The latter coefficients as functions of the drift angle β and modified non-dimensional yaw velocity Ω_m are next stored in lookup tables (matrices). a discretisation step of 10° is chosen for β, while Ω_m is spaced at: 0.0000, 0.4472, 0.7071, 0.8321, 0.8944, 0.9285, and 0.9707.

Fig. 2 presents a correlation (restrictions made to possible combinations) between β and Ω_m existing in five manoeuvres to be investigated in the present study- two turning tests (full and half ahead speed, 35° and 65° rudder respectively), and three z-tests (10°/10° and 20°/20°, both at full ahead throttle, and 20°/20° executed at dead slow ahead speed).

It is obvious from Fig. 2 that only those nodes (elements) in the c_{fyhm} and c_{mzhm} lookup tables may be at the most precisely identified (calibrated) which are directly adjacent to the β-Ω_m sea trial trajectories. For other regions of β-Ω_m another manoeuvring trials are desired. This should be kept in mind because the initial guess, e.g. (16), and the tuning method (introduced later) principally rely however on the whole β-Ω_m range. The initial estimates of c_{fyhm} and c_{mzhm} by (16) are displayed in Figs. 3 and 4 ('initial').

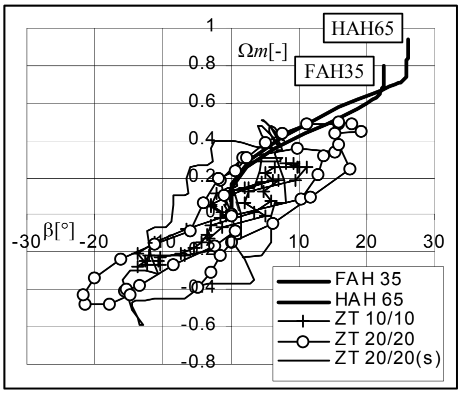

Fig. 2. Correlation among drift angle and yaw non-dimensional velocity

IDENTIFICATION OF HULL HYDRODYNAMIC EXCITATIONS

The proposed new method, though relatively very simple in the concept, gives a huge advance over the author's previous attempts, e.g. [Artyszuk, 1999], [Artyszuk, 2003a], and different manoeuvring model parametric optimisation encountered elsewhere in the open literature, and over some optimisation runs made by the author's himself too.

In case of many model parameters to be adjusted at the same time, any optimisation is a long-time lasting process, and often guaranteeing no success. The reasons are quite miscellaneous: a bad selection of parameters, a low adequacy of the model structure, an improper variation range for parameters, imperfect criteria of convergence (i.e. for a particular motion variable, for all three manoeuvring motions together - weighing factors required, and finally among different manoeuvres engaged in the identification). In such circumstances the point is that the mathematically best fit does mean to be physically verifiable. The above problems explicitly regard also the complex lookup table-stored functional relationships for c_{fyhm} and c_{mzhm}.

From the comprehensive sea trials program, five manoeuvring tests have been selected for the below identification as stated before. They consist of two turning tests, which constitute a primary data source, and three zigzag tests, treated hereafter as a supplementary data.

The importance and quality of the turning tests lies in their ability to be well post-processed in view of random errors (data smoothing, [Artyszuk, 2000]) or systematic biases due to the sea current presence (allowances for sea current, e.g. [Artyszuk, 2001c]).

The complete and newly refined smoothed data of the full ahead 35° and half ahead 65° turning manoeuvres of the chemical tanker are included further in Figs. 8 and 9 ('trial').

The basic principle of the proposed identification is a possession of knowledge on all three motion parameters completely describing the ship manoeuvring. Those are essentially: surge, sway, and yaw velocities (v_x, v_y, ω_z) directly standing in eqs. (1). Anyhow, other equivalent combinations of any three independent kinematic variables may exist for an arbitrary ship in sea trials, e.g. time series of (v_{xy}, β, ω_z) or (x_0, y_0, ψ), which can be however numerically converted, more or less accurately, to the three velocities and their corresponding derivatives.

Since a direct analysis of the surge velocity behaviour is very hard and often confusing (the surge motion equation is too 'sensitive'), a ship manoeuvring auxiliary model has been composed, which predicts sway v_y and yaw ω_z velocities based on the supplied sea trial data on surge velocity v_x (the surge equation in (1) does not evolve). Additionally, either trial data on v_y or trial data on ω_z may be embedded in the model resulting in one differential equation to be solved only.

For simplicity and pictorial purposes (the identification is not yet fully automated), the analysis of β and Ω_m (which are also placed in c_{fyhm} and c_{mzhm}) is performed instead of v_y and ω_z.

Because the FAH 35° and HAH 65° turnings indicate a rapid increase of β and Ω_m, which can not be straightforwardly achieved (in view of the adopted rudder hydrodynamics) by reasonable lowering the hull sway force and yaw moment coefficients (as initially estimated), the rudder force augmenting factor a_H equal to $\underline{0.6}$ is taken as the reference (in the literature values of order 0.4 are usually found).

The other hull-rudder interaction parameter, namely c_{12} ('responsible' for the rudder lateral inflow) is assumed at the opening level $\underline{0.8}$.

The main objective is now to so adjust the hull hydrodynamic coefficients $c_{fyhm}(\beta, \Omega_m)$ and $c_{mzhm}(\beta, \Omega_m)$, strictly the appropriate elements (nodes) of the corresponding lookup tables, as to reach the best least-square convergence of the simulated and trial drift angles (β) or non-dimensional yaw velocities (Ω_m). This is to be done in two steps i.e. independently for c_{fyhm} and c_{mzhm}. Firstly, the hull sway force coefficient is being identified through substituting trial values of ω_z (in both turnings) into the sway equation of (1). Thus only one variable is free in the behaviour, namely v_y (or β), while all others are absolutely accurate.

Tab. 2, besides the final multipliers to be applied to the initial guess (Fig. 3, 'initial') for the best convergence results, has four emphasised areas which roughly indicate the regions of β-Ω_m connected with the 10°/10° z-test, 20°/20° z-test, 35° turn test, and 65° turning manoeuvre respectively.

The tuning of the c_{fyhm} is sequential, i.e. starting from the first element (β=0, Ω_m=0), a move is made (strictly following the increasing drift angles in both FAH 35° and HAH 65° up to their steady phases) through the adjacent regions in the manner the whole row (Ω_m=const) or the whole column (β=const) may be changed at once, but the independent calibration of an element at the row/column intersection is allowed too. As can be seen from Tab. 2, the third region (β=30°, Ω_m=0.8321) for example consists of one row and one column, thus only three degrees of freedom exist (three distinct values). An exception is here the last region, inherent to the 65° turn test modelling, where the last column is free to change. Though the drift angle of HAH 65° is between 20° and 30°, tuning only the column at 30° is better justified in the light of some scale model tests.

This way, the identification of a region next in turn (higher values of β and Ω_m) does not affect previous regions (lower values of β and Ω_m). One more rule of the recommended identification is that, if the convergence effect is small in magnitude when compared to the magnitude of the adjustment, such table nodes are not tuned up.

The mentioned least-square convergence criterion does not apply to the whole curve of the drift angle, but to particular partial regions of β-Ω_m in Tab. 2.

The final chart of c_{fyhm} is shown in Fig. 3 ('adjusted'). a similar procedure to the above is to be implemented for the hull yaw coefficient $c_{mzhm}(\beta, \Omega_m)$. Anyhow, the yaw motion equation (ω_z) of (1) is a 'locomotive' here, into which the trial data on v_y have been incorporated by analogy.

The ultimate correction multipliers for c_{mzhm} are gathered in Tab. 3., and the new c_{mzhm} chart is illustrated in Fig. 4 ('adjusted'). For comparison purposes, Figs. 3 and 4, include also estimates of the hull hydrodynamic coefficients according to [Inoue et al., 1981] ('Inoue') and [Kijima et al., 1993] ('Kijima').

Table 2. Correction multipliers for c_{fyhm}.

Ω_m[-]\β[°]	0	10	20	30
0.0000	1.0	0.5	0.7	1.0
0.4472	1.0	0.5	0.7	1.0
0.7071	1.1	1.1	0.7	1.0
0.8321	1.0	1.0	1.0	1.5
0.8944	1.0	1.0	1.0	1.8
0.9285	1.0	1.0	1.0	2.0
0.9701	1.0	1.0	1.0	2.2

Table 3. Correction multipliers for c_{mzhm}.

Ω_m[-]\β[°]	0	10	20	30
0.0000	1.0	1.8	1.8	1.4
0.4472	1.8	1.8	1.8	1.4
0.7071	1.8	1.8	1.3	1.4
0.8321	1.1	1.1	1.1	1.4
0.8944	1.0	1.0	1.0	1.0
0.9285	1.0	1.0	1.0	1.0
0.9701	1.0	1.0	1.0	1.0

The convergence of β and Ω_m for both turnings is demonstrated in Figs. 5 and 6, which is rather successful, while at the same time the correction multipliers of Tabs. 2 and 3 keep within reasonable limits.

At the present stage of research, the z-test data do not intend to influence (participate in) the calibration of the hull hydrodynamic coefficients c_{fyhm} and c_{mzhm}. Because, notwithstanding some advantages, they could sometimes 'distort' the previously identified data. This is a very important restriction, since the simulation of z-tests is also sensitive to a_H and c_{12} estimates, which will be proved later.

Just for a closer look inside, the prediction of β and Ω_m in z-tests, based on substituted trial data (however without any post-processing as usual for the turning tests) of v_x and ω_z for the former variable, or v_x and v_y for the latter one, is displayed in Fig. 7. The already identified (through turning tests) hull hydrodynamic coefficients are utilised here.

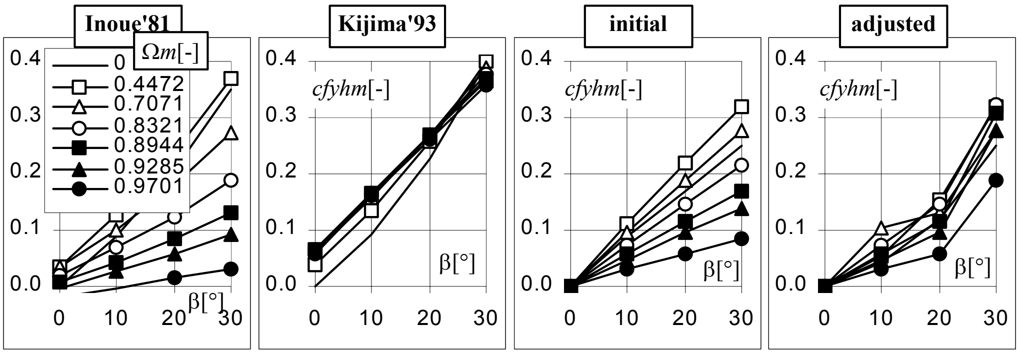

Fig. 3. Hull sway force coefficients

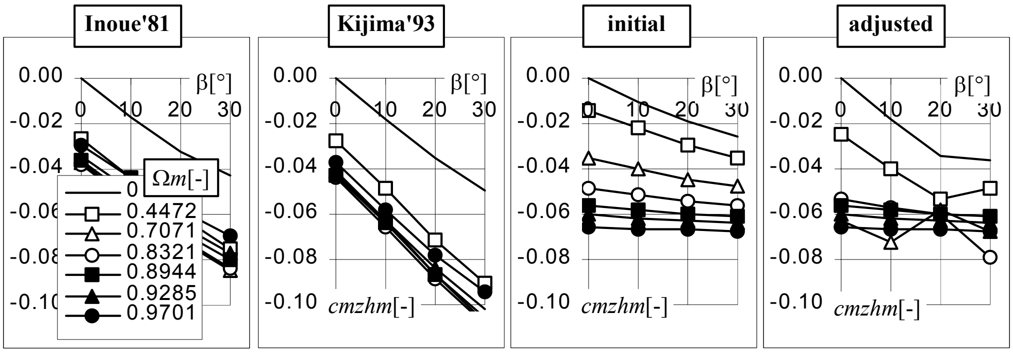

Fig. 4. Hull yaw moment coefficients

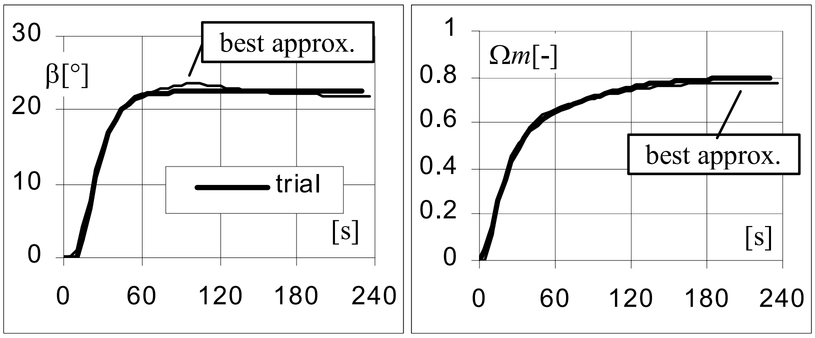

Fig. 5. Results of model independent tune-up vs. drift (left) and yaw (right) - FAH 35°

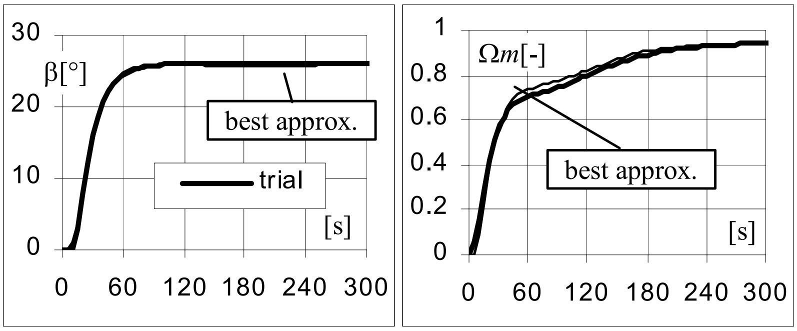

Fig. 6. Results of model independent tune-up vs. drift (left) and yaw (right) - HAH 65°

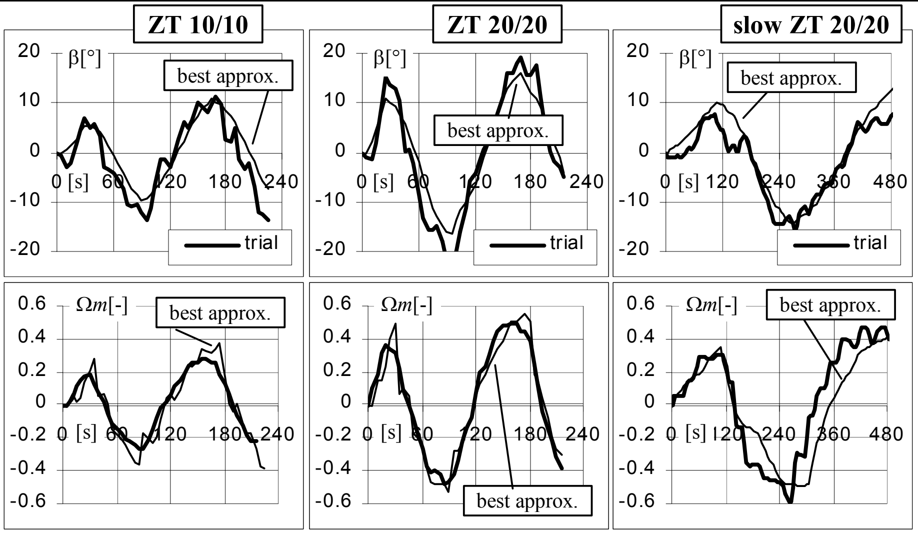

Fig. 7. Effect of FAH 35°/HAH 65°-based model independent identification upon z-tests.

FINAL SIMULATION AND SENSITIVITY ANALYSIS

The most interesting is now how the manoeuvring model (1) under known c_{fyhm} and c_{mzhm} lookup tables will normally perform when all three manoeuvring velocities are free in changing. The overall ship manoeuvring simulation is shown in Figs. 8 and 9. The agreement vs. sea trials is more than satisfactory.

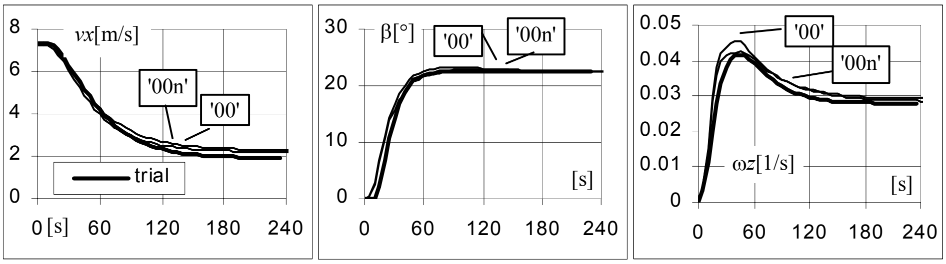

Fig. 8. Final FAH 35° simulation (all motion variables free)

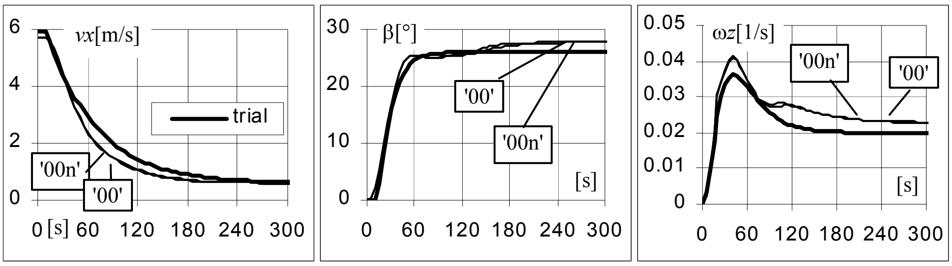

Fig. 9. Final HAH 65° simulation (all motion variables free)

Figs. 10 and 11 present a sensitivity analysis of the FAH 35° and HAH 65° turning tests for a_H and c_{12} being much varied from the initial conditions. The symbols used in Figs. 8 to 11, and in further ones, are defined in Tab. 4.

Table 4. Naming convention.

model release	a_H	c_{12}	remarks
'00'	1.6	0.8	initial conditions
'00n'	1.6	1.0	final conditions
'11'	1.2	0.5	
'12'	1.2	1.1	
'21'	2.0	0.5	
'22'	2.0	1.1	

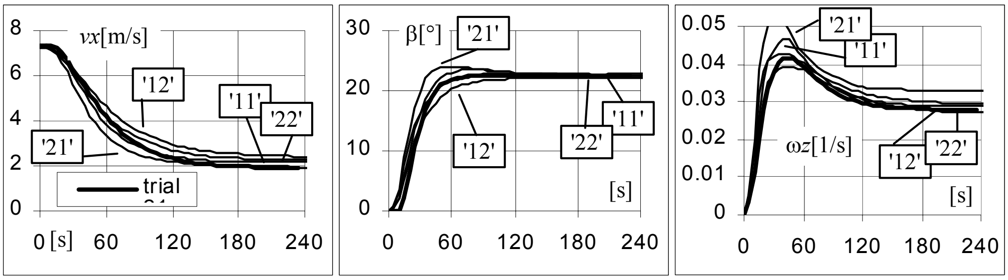

Fig. 10. Model output sensitivity on rudder related coefficients - FAH 35°

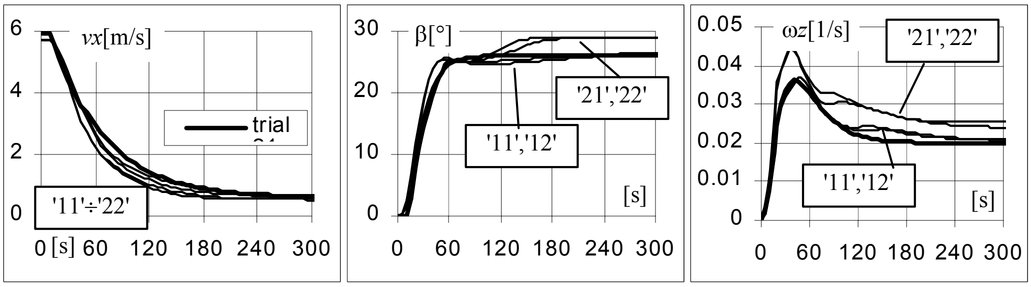

Fig. 11. Model output sensitivity on rudder related coefficients - HAH 65°

The overall simulations of z-tests are included in Figs. 12-15, which enable in certain limits to select a proper combination of a_H and c_{12}.

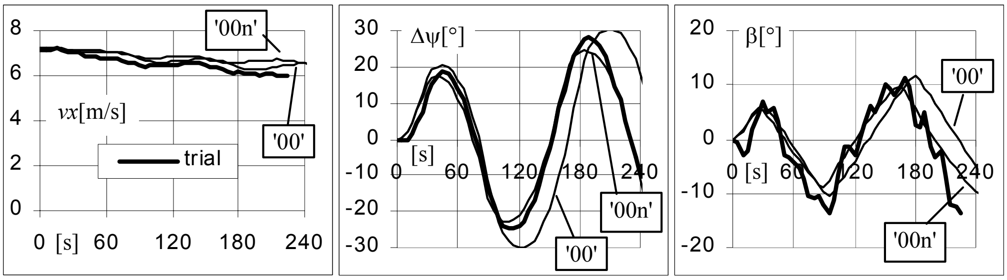

Fig. 12. Final ZT 10°/10° simulation (all motion variables free).

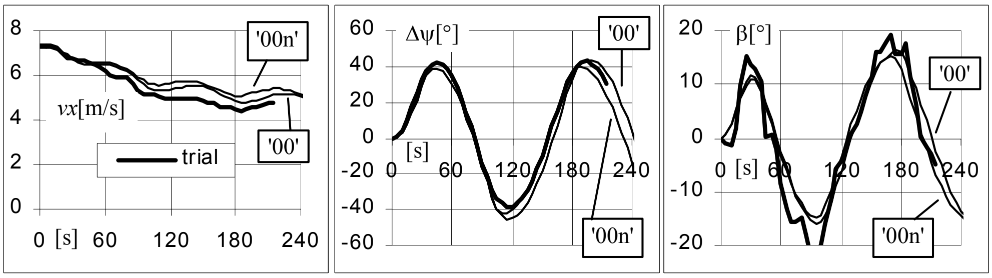

Fig. 13. Final ZT 20°/20° simulation (all motion variables free)

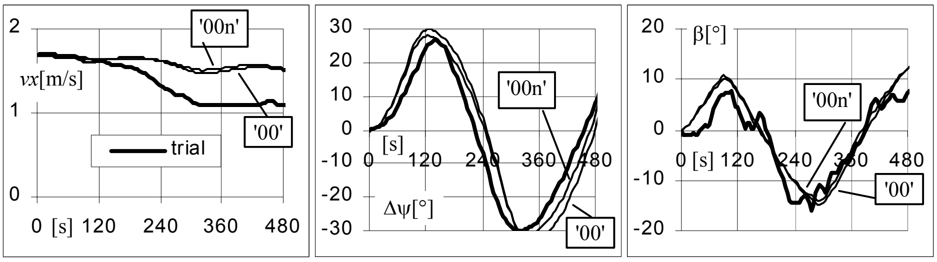

Fig. 14. Final slow speed ZT 10°/10° simulation (all motion variables free)

It appears that the convergence of all three z-tests at the standard (a_H, c_{12}) values (1.6 and 0.8 respectively, '00') is generally good, Figs. 12 to 14, though a bit better performance is reached when c_{12} is slightly increased up to 1.0 ('00n').

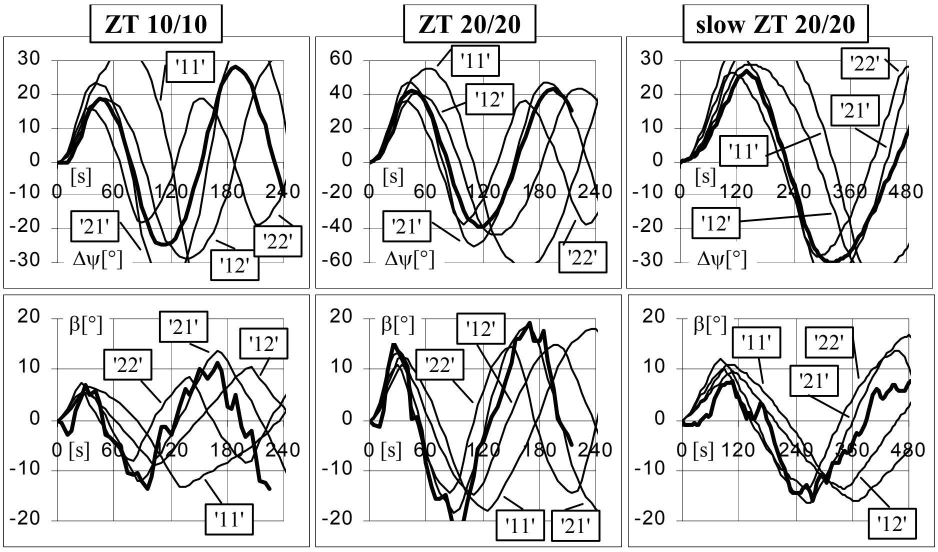

Fig. 15. Model output sensitivity on rudder related coefficients - z-tests

The consequences of choosing particular values of a_H or c_{12} are well visible in a spiral test simulation- Figs. 16 and 17. It is a pity that this manoeuvre was not executed during the sea trial program. At the initial values of (a_H, c_{12}), the ship experiences in the simulation a small yaw instability loop, which would be minimised with the increasing c_{12} ('00n'), ensuring in our case also the best prediction of z-tests.

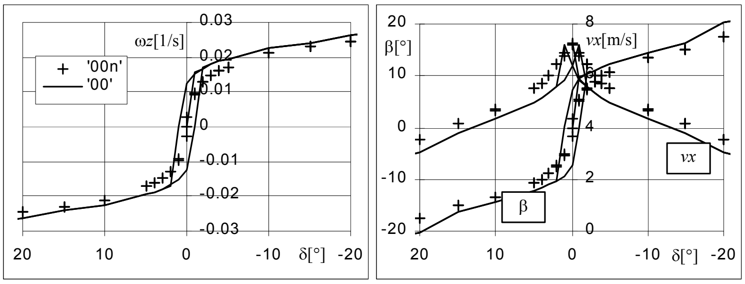

Fig. 16. Final simulation of spiral test (all motion variables free)

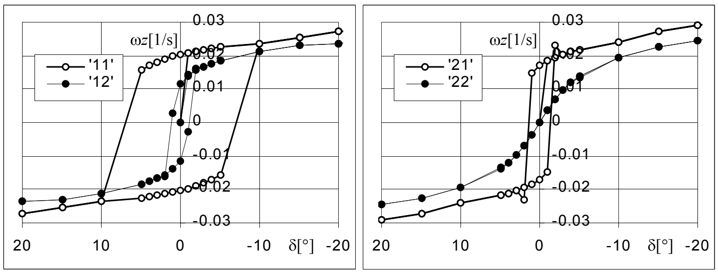

Fig. 17. Model output sensitivity on rudder related coefficients - spiral test

It can be concluded that, though z-tests comprise to some extent a 'behaviour' of the spiral test, nothing is however quantitatively clear whether e.g. this or that overshoot angle in the ship heading causes or not any instability loop in the spiral test. The spiral test shall be deemed as a supplementary and necessary manoeuvre.

We could only believe that there is no yaw instability for the chemical tanker being investigated, but this can not be considered as granted.

FINAL REMARKS

The present study quantitatively revealed that the ship manoeuvring behaviour during turning is really mostly governed by the hull hydrodynamic forces (see the low sensitivity of simulation upon a_H and c_{12}). On the other hand, due to relatively small drift angles and yaw velocities involved, a prediction of z-tests is more prone to these rudder-related coefficients.

Those two facts shall be remembered while making a further improvement and development of the ship manoeuvring identification procedure described above. Providing here (as one more evidence) charts of a percentage distribution of the total external excitations among the hull and rudder would unnecessarily extend the volume of the paper.

There are still many questions and problems to answer of course, e.g. whether the rudder force sub-model has to be accurately or may be just roughly assessed in view of its effect upon the final manoeuvring simulation. The latter aspect is very important because of the assumptions made to the rudder lift/drag diagrams (Fig.1) and a_H or c_{12} as constants.

Furthermore, the weakest link of the recommended identification procedure is an ambiguity in the lookup tables of c_{fyhm} and c_{mzhm}, which may be accidentally introduced into them while the least-square tuning stage.

NOMENCLATURE

a_H	- rudder force augmenting factor	T	- ship draft
A_R	- rudder area	T_P	- propeller pure thrust
B	- ship breadth	v_p	- propeller advance velocity
c_{12}	- rudder lateral flow correction factor	v_R	- rudder effective flow velocity
c_B	- hull block coefficient	v_x	- ship surge velocity
c_D , c_L	- rudder drag/lift coefficients	v_{xy}	- ship total linear velocity
c_{fxh} , c_{fyh} , c_{mzh}	- hull surge/sway force and yaw moment coefficients	v_y	- ship sway velocity
c_{fxhm} , c_{fyhm} , c_{mzhm}	- a/a but modified	v_{yR}	- rudder flow effective lateral velocity
c_m	- m_{22} ratio in surge equation	x_0 , y_0	- ship earth-related position in
c_{Th}	- propeller thrust load ratio	x_R	- rudder abscissa (negative)
D	- propeller diameter	w	- propeller wake fraction
F_{DR} , F_{LR}	- rudder drag/lift forces	α	- rudder effective incidence angle
F_x , F_y , M_z	- external excitations	β	- hull drift angle
J_m	- propeller modified advance ratio	β_R	- rudder effective local drift angle
J_z	- ship moment of inertia	δ	- rudder deflection angle (port positive)
k_{tm}	- propeller thrust coefficient	λ	- rudder aspect ratio
L	- ship length	ρ	- water density
m	- ship mass	ω_z	- ship yaw velocity
m_{11} , m_{22} , m_{66}	- surge/sway/yaw added masses	$\overline{\omega_z}$	- ship yaw relative velocity
n	- propeller revolutions	Ω_m	- a/a but modified
n_n , P_{En}	- main engine rpm/power	ψ	- ship heading
P/D	- propeller pitch ratio	H , P , R	- hull, propeller, rudder indices
t	- propeller thrust deduction		

REFERENCES

1. Artyszuk J., Dynamics-Based Identification of Ship Motion Mathematical Model from Full-Scale Trials Results. Annual of Navigation, no. 1/99, Polish Academy of Sciences/Polish Navigation Forum, Gdynia, 1999.
2. Artyszuk J., Data Smoothing Application to the Ship Motion Mathematical Model Identification. Annual of Navigation, no. 2/00, Polish Academy of Sciences/Polish Navigation Forum, Gdynia, 2000.
3. Artyszuk J., a Structural Identification of the Ship Manoeuvring Motion Mathematical Model. HYDRONAV '2001, 14th International Conference on Hydrodynamics in Ship Design, Sep 27-29, Szczecin-Miedzyzdroje, 2001a.

4. Artyszuk J., Full-scale Trials and Rudder Hydrodynamics of a Schilling Rudder Ship. HYDRONAV 2001, 14th International Conference on Hydrodynamics in Ship Design, Sep 27-29, Szczecin-Miedzyzdroje, 2001b.
5. Artyszuk J., Some Problems of Ship Manoeuvring Motion Dynamics Identification from Full-Scale Trials. 1st International Congress on Maritime Transport 'Maritime Transport 2001', Proceedings ('Maritime Transport'), Nov 21-23, Barcelona, 2001c.
6. Artyszuk J., Rudder Local Drift Angle during Ship Manoeuvring Based on Full Scale Trials. Scientific Bulletin 'Transport' no. 1(15), TransComp '02, 6th Conference on 'Computer Systems for Supporting Research, Industry and Transport', Dec 4-6, Technical University of Radom, Zakopane, 2002.
7. Artyszuk J., Practical Aspects of Lookup Tables Identification in Case of Ship Manoeuvring. Scientific Bulletin, no.21 (Applied Mechanics 2003 Conference, Jaworzynka, Mar 24-26), Silesian University of Technology, Department of Applied Mechanics, 2003a.
8. Artyszuk J., Ship Sway/Yaw Motions while Turning with Bow Lateral Thruster. To be presented at 15th International Conference on Hydrodynamics in Ship Design, Safety and Operation, HYDRONAV '2003, Gdansk, Oct 22-24, 2003b.
9. Inoue S., Hirano M., Kijima K., Hydrodynamic Derivatives on Ship Manoeuvring. International Shipbuilding Progress (ISP), vol. 28, no. 321 (May), 1981.
10. Kijima K., Tanaka S., Furukawa Y., Hori, T., On a Prediction Method of Ship Manoeuvring Characteristics. MARSIM '93 Proc., vol.1, International Conference on Marine Simulation and Ship Manoeuvrability, Sep 26-Oct 2, St. John's, 1993.
11. Ruseckij A.A., Controllable Pitch Propeller Hydrodynamics. Sudostroenie, Leningrad, 1968 (in Russian).

Received September 2003
Reviewed November 2003